


FULL PAPER

Open Access



A low-energy particle experiment for both ion and electron measurements using a single microchannel plate-based detector

Shoichiro Yokota^{1*} , Yoshifumi Saito² and Kazushi Asamura²

Abstract

We have developed a low-energy particle experiment that alternately measures ions and electrons in space. The ability to switch between ion and electron measurements is achieved by simply adding ultra-thin carbon foils and positive and negative outputs to a conventional top-hat electrostatic analyzer and a high-voltage power supply, respectively. The advantage of this experiment is that it can perform both ion and electron measurements using only one MCP-based detector for electrons, since it detects secondary electrons emitted from the carbon foils. For the SS520-3 sounding rocket program, we prepared two identical energy analyzers, one for ions and the other for electrons to demonstrate this technique. Laboratory tests confirmed that the performance of the two analyzers was comparable to that of conventional analyzers for ion and electrons. The SS520-3 rocket experiment in the high latitude auroral region yielded observations that captured typical features of ions and electrons, which were similar to previous observations.

Keywords Electrostatic analyzer, Space plasma measurements, SS520-3 sounding rocket, Ion and electron measurements, Microchannel plate

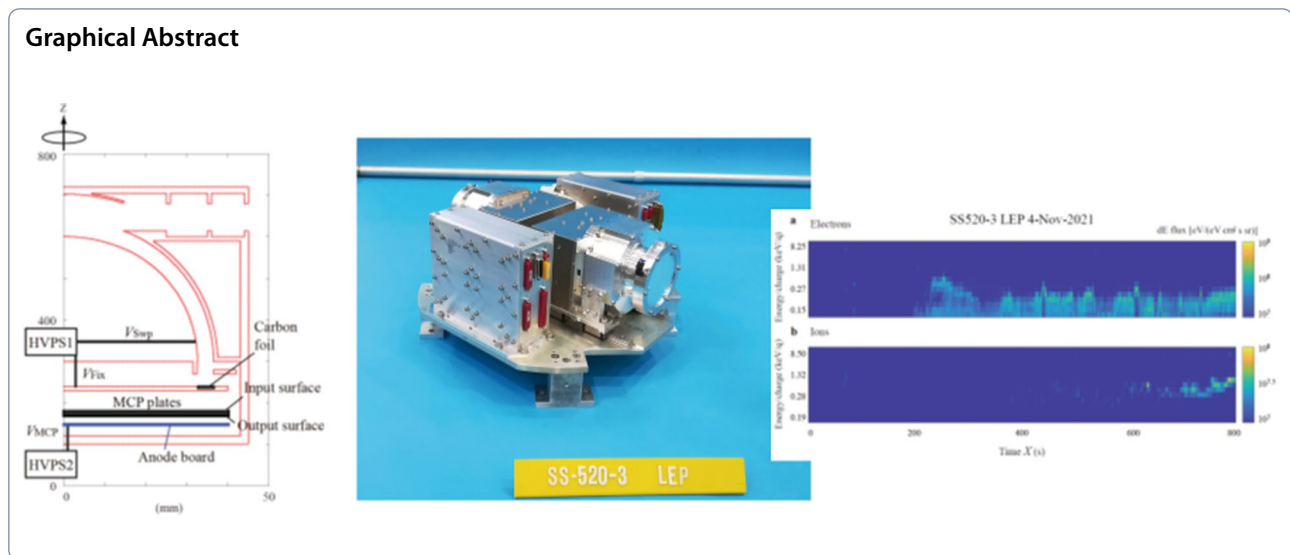
*Correspondence:

Shoichiro Yokota
yokota@ess.sci.osaka-u.ac.jp

Full list of author information is available at the end of the article



© The Author(s) 2024. **Open Access** This article is licensed under a Creative Commons Attribution 4.0 International License, which permits use, sharing, adaptation, distribution and reproduction in any medium or format, as long as you give appropriate credit to the original author(s) and the source, provide a link to the Creative Commons licence, and indicate if changes were made. The images or other third party material in this article are included in the article's Creative Commons licence, unless indicated otherwise in a credit line to the material. If material is not included in the article's Creative Commons licence and your intended use is not permitted by statutory regulation or exceeds the permitted use, you will need to obtain permission directly from the copyright holder. To view a copy of this licence, visit <http://creativecommons.org/licenses/by/4.0/>.



Introduction

Since the beginning of space faring many space-born plasma observation programs have been carried out. Advances in plasma measurement technology and space plasma research have expanded the observation area from the near-Earth space to other planets, moons, and small bodies (Pfaff et al. 1998). The primary requirement for in situ observations of the space plasma is to obtain velocity distribution functions of ions and electrons with appropriate resolution.

Since its development (Carlson et al. 1982; Young et al. 1988), the top-hat electrostatic analyzer (ESA) has become a standard instrument for recent space plasma observation missions such as Arase and BepiColombo/Mio (e.g., Asamura et al. 2018; Yokota et al. 2017; Saito et al. 2021), because its axisymmetric shape provides uniform performance in all directions in principle, and high sensitivity with relatively small resources. If the spinning motion of the spacecraft is not used to acquire a field of view (FOV) in all directions, there is an option to extend the FOV with deflectors at the entrance of the analyzer (e.g., Pollock et al. 2016; Yokota et al. 2005; Yokota et al. 2021; Kasahara et al. 2023).

Because future space plasma measurements will require multi-point observations using small satellites and even CubeSats, the most important issue is to develop low-resource experiments. One low-resource solution is the combination of ion and electron analyzers. In exploration programs such as Rosetta (Burch et al. 2007), THEMIS (McFadden et al. 2008), and Parker Solar Probe (Kasper et al. 2016), and the ocean topography mapper JASON-3 (Sauvaud et al. 2018), resources were reduced by placing the two top-hat ESAs in close proximity and by sharing an electronics box.

Another solution is a specially shaped ESA, with an increased number of spherical/toroidal shell electrodes to analyze ions and electrons simultaneously and/or multiple energy bands (Frank et al. 1992; Morel et al. 2016; Ogasawara et al. 2018; Su et al. 2022; Hirahara et al. 2023). Although all of these are effective in reducing the resources required for plasma analyzers, the issue remains that they require two different types of micro-channel plate (MCP)-based detectors, one for ions and the other for electrons. It should be noted that the function to switch between electron and ion measurements is implemented by the two instruments of the Particle Environment Package for the JUICE mission (Galli et al. 2022, Barabash et al. 2013).

In this article, we present a low-energy particle (LEP) experiment that can measure both ions and electrons in the same configuration by adding an ultra-thin carbon foil between the top-hat ESA and the MCP-based detector. The MCP-based detector for electrons is used for both ion and electron measurements because it detects secondary electrons emitted from the carbon foil by incident ions or electrons. It should be noted that the high-voltage power supply (HVPS) for the ESA additionally requires the ability to switch between positive and negative output polarity. The LEP experiment measures ions and electrons not simultaneously, but alternately according to the polarity switching of the HVPS. From the next section, we describe the instrumentation of the LEP experiment and show the results of simulations and laboratory experiments.

The LEP experiment was installed on the SS520-3 sounding rocket and successfully acquired observation data during its flight on November 4, 2021. Therefore, the

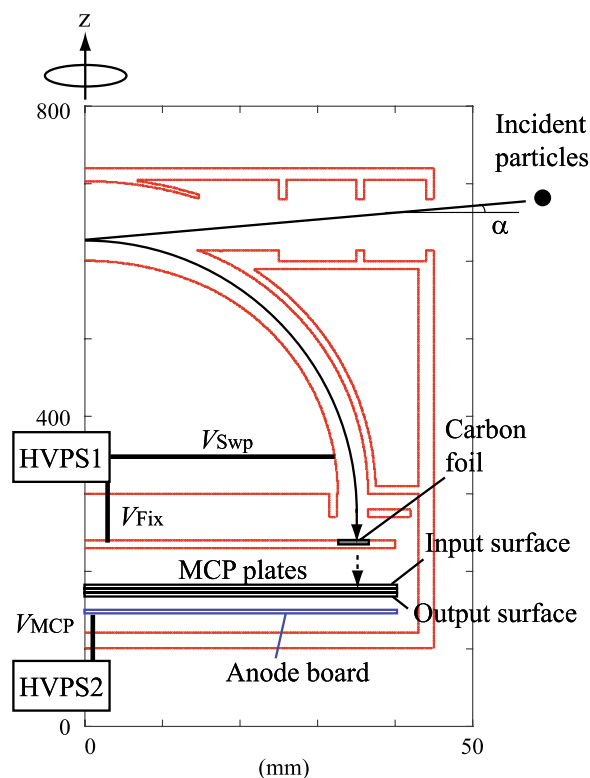


Fig. 1 Cross-sectional view of the ion optics and MCP-based detector in the LEP experiment. The solid arrow indicates the trajectory of incident particles at elevation α move through the ESA and into the MCP-based detector at the bottom. The dashed arrow indicates the trajectories of secondary electrons emitted from the carbon foil. HVPS1 and 2 supply V_{Swp} and V_{Fix} , and V_{MCP} , respectively

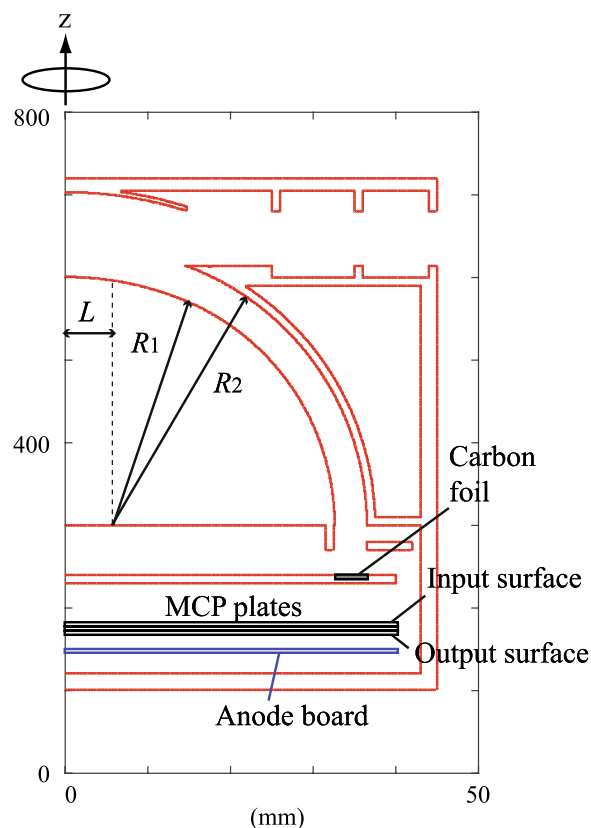


Fig. 2 Dimensions of the ion optics in the LEP experiment

observation data are also presented to demonstrate the practicality of the LEP experiment.

Instrumentation

Design concepts

Figure 1 shows the ion optics of the LEP experiment for both ion and electron measurements. Incident ions/electrons are energy selected by the top-hat ESA and move to the detector at the bottom, when the inner spherical electrode of the ESA is applied with a sweeping negative/positive high voltage $-V_{Swp} / +V_{Swp}$ by HVPS1.

The top-hat ESA is the same geometry as that of the low-energy electron spectrometers developed for the ICI-2-4 sounding rockets (Spicher et al. 2016), with toroidal electrodes of $R_1=29.5$ mm, $R_2=33.5$ mm, and $L=3.0$ mm, as shown in Fig. 2. The difference to the electron spectrometers on the ICI rockets is that between the ESA exit and the MCP-based detector an ultra-thin carbon foil is inserted. The MCP-based detector consists of z-stack MCP plates and an anode

board. Photographs of all components of the LEP experiment are shown in Fig. 3.

MCP-based detectors are sensitive to ions above a few kiloelectronvolts and to electrons above relatively low energies (Fraser 2002 and references therein). In addition, MCP-based detectors require a bias voltage to amplify secondary electrons. Therefore, to measure ions and electrons above a few electron volts, a negative voltage of -2 to -3 kV is typically applied to the input surface of the MCP plates for ions, with a negative potential of a few hundred volts on the output face, and a positive voltage of $+2$ to $+3$ kV is applied to the output surface (or a neighboring anode plate) for electrons, with a positive potential of a few hundred volts on the input face (e.g., Pollock et al. 2016). In short, the MCP-based detectors for ions and electrons require different high-voltage distributions.

The MCP-based detectors of the LEP experiment can in principle be substituted by the Channel electron multiplier (CEM)-based detectors, while the CEM-based detectors also require different high-voltage distributions for the ion and electron measurements. Because of the simpler structure and lower resources

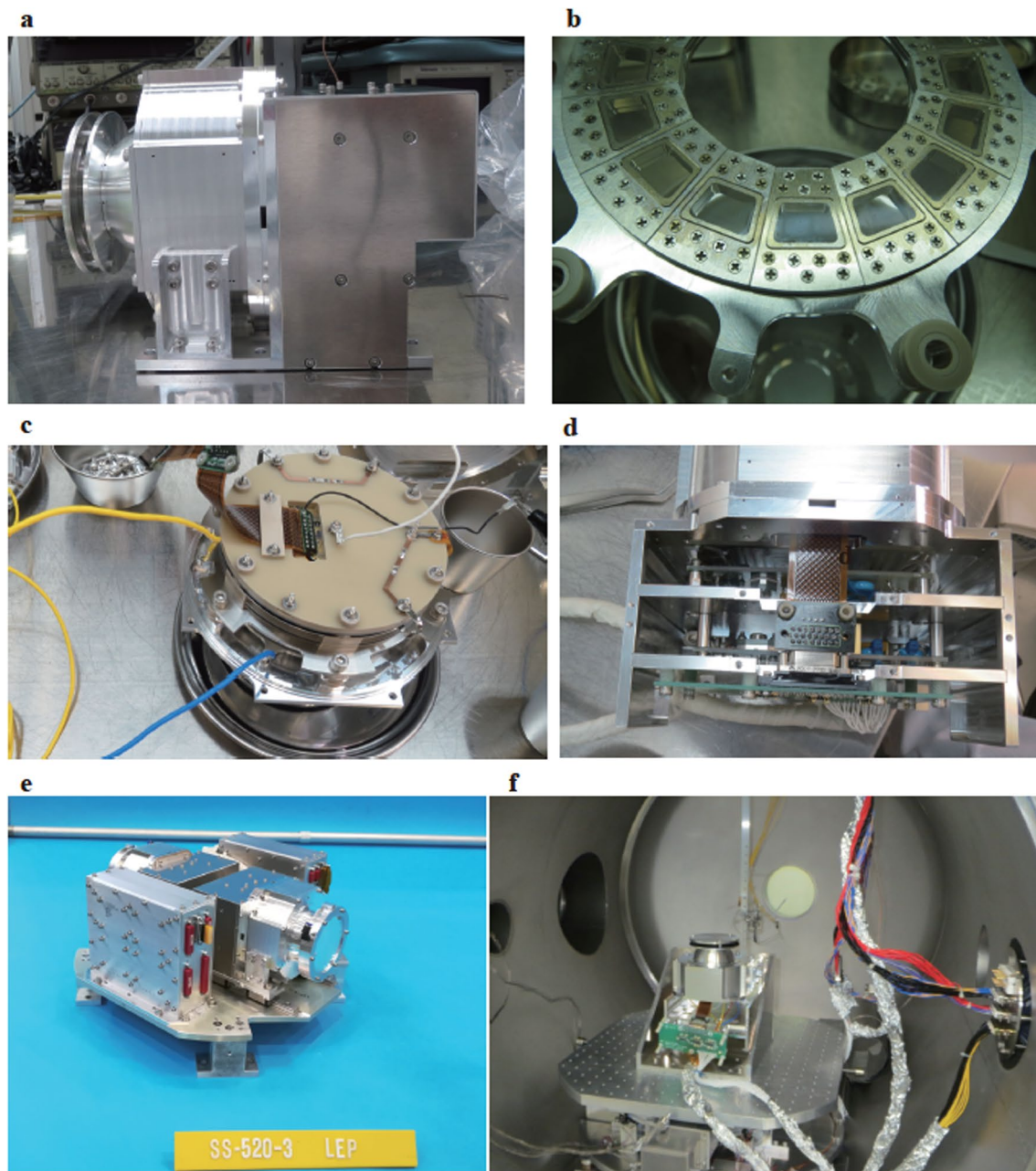


Fig. 3 Photographs of the LEP experiment for the SS520-3 sounding rocket. **a** Sensor unit. **b** Carbon foil plate in the sensor unit. **c** MCP-based detector in the sensor unit. **d** HVPS box in the sensor unit. **e** The entire components of the LEP experiment on the instrument panel. **f** Sensor unit in a vacuum chamber for performance test

when combined with the top-hat ESA, we employed the MCP-based detector for the LEP experiment.

When the LEP experiment measures ions, a sweeping negative voltage $-V_{\text{Swp}}$ is applied to the inner toroidal electrode of the ESA and a fixed negative voltage $-V_{\text{Fix}}$ is applied to the carbon foil to increase the ion transmission rate (see Fig. 1). Since HVPS1 originally

holds $-V_{\text{Fix}}$ inside the circuit to output $-V_{\text{Swp}}$, where $V_{\text{Fix}} = \max V_{\text{Swp}}$, $-V_{\text{Fix}}$ can be supplied from HVPS1, without additional HVPS resources. In the case of electron measurements, the polarity is reversed, and as in the case of ion measurements, a single HVPS provides sweeping and fixed positive voltages, $+V_{\text{Swp}}$ and $+V_{\text{Fix}}$, to the inner electrode of the ESA and the carbon foil, respectively (Additional file 1: Fig. S1).

Using the carbon foil as shown in Fig. 1, both ion and electron measurements can be performed with a single MCP-based detector for electrons. A fixed positive high voltage V_{MCP} is applied to the anode board of the MCP-based detector, and a moderate bias voltage is distributed to the MCP plates by a voltage divider. It should be noted that an electric potential higher than that of the carbon foil is required at the input surface of the MCP plates to carry secondary electrons emitted from the carbon foil to the MCP plates.

Another point to emphasize is that the energy of secondary electrons detected by the MCP-based detector is determined almost exclusively by the potential difference between the input surface of the MCP plates and the carbon foil. Although the MCP detection efficiency depends on the incident particle energy (e.g., Fraser 2002), the MCP-based detector in the LEP experiment measures secondary electrons of the same energy for incident particles of any energy. Therefore, the LEP experiment is expected to have a smaller energy dependence than conventional plasma analyzers. It should be noted that at incident energies above 2 keV, the transmittance of H^+ and He^+ through the 5 nm carbon foil can be considered constant (>99% and >97%, respectively), while the energy dependence of O^+ transmittance cannot be neglected (58, 89, and 98% at 2, 4, and 8 keV, respectively), according to the Stopping and Range of Ions in Matter (SRIM) model (Ziegler 2004). Incident ions suffer energy dispersion and angular scattering at the carbon foil, but this is not relevant to the subsequent secondary electron measurement.

The LEP experiment for the SS520-3 sounding rocket program

The SS520-3 sounding rocket program of the Institute of Space and Astronautical Science (ISAS) has planned to investigate the ion acceleration/heating mechanism in the cusp region. The observation experiment with the SS520-2 sounding rocket was conducted at the same launch site (Tanaka et al. 2003) with the same objectives. Based on the experience in developing ion and electron spectrometers for the SS520-2 sounding rocket program, we developed the LEP experiment on the SS520-3 sounding rocket.

Figure 3 shows photographs of the LEP experiment. The sensor unit, consisting of two HVPS boards in addition to the top-hat ESA, carbon foil plate, and MCP-based detector is shown in Fig. 3a. The approximately 5-nm thick carbon foil is on a 333 lines per inch metal grid, with 16 holders mounted circumferentially on a single plate, as shown in Fig. 3b. Although a thinner carbon foil is available, 5-nm carbon foils were chosen for ease of handling. Even at 5 nm thickness, sufficient transmittance can be achieved at the applied voltage planned to

be used as described below. The MCP-based detector is mounted directly under the carbon foil plate (see Fig. 3c). Two HVPS boards which supply high voltages to the top-hat ESA and MCP-based detector are shown in Fig. 3d. The only difference from the electron spectrometer for the ICI rockets is the addition of the carbon foil plate in Fig. 3b.

The entire LEP experiment mounted on the instrument panel is shown in Fig. 3e, which consists of two sensor units and one electronics box for control and handling the observation data. The panel has two electronics boxes, one of which belongs to another experiment that will be mounted below the LEP experiment in the rocket payload. The two sensor units are mounted on rails because they move outward after launch to ensure clearance of the FOV (see Fig. 3e). In the performance test, the sensor units were placed one by one on a turntable in a vacuum chamber to acquire their characteristics using ion beams, as shown in Fig. 3f.

The anode board of the MCP-based detector in Fig. 3c contains the electrodes of the 64-discrete anodes, and an application specific integrated circuit (ASIC) chip including 64-channel amplifiers, discriminators, and counters (Saito et al. 2017). The anode board has 64 channels for 360° azimuthal coverage but due to data limitations on the SS520-3 program the telemetry must be reduced. This is achieved by combining four adjacent channels into one, resulting in 16 channels total.

The science objectives of the SS520-3 program are to investigate the ion acceleration/heating mechanism in the cusp region, similar to observation experiments of the ICI and SS520-2 rocket programs (Spicher et al. 2016; Tanaka et al. 2003). Thus, the performance requirements such as the energy range below 10 keV are the same as these experiments. For the SS520-3 program, two identical sensor units were prepared, one for ions and the other for electrons. As a result, since there is no need for a HVPS capable of bipolar output for $\pm V_{\text{SWP}}$ and $\pm V_{\text{FIX}}$, an HVPS that outputs only negative polarity for $-V_{\text{SWP}}$ and $-V_{\text{FIX}}$ was installed in the sensor unit for ions, and another HVPS that outputs only positive polarity for $+V_{\text{SWP}}$ and $+V_{\text{FIX}}$ was in the sensor unit for electrons. The development of the bipolar HVPS remains a future issue.

To observe ions and electrons below 10 keV in the SS520-3 program, the maximum voltages for the inner ESAs are 2 kV ($V_{\text{SWP}} \leq 2$ kV), and as a result, fixed voltages of 2 kV are applied to the carbon foil plate ($V_{\text{FIX}} = 2$ kV). Since 2.6 kV was required as the bias voltage for the MCP plates, the anode board of the MCP-based detector in the sensor unit for electrons was applied with +4.9 kV ($V_{\text{MCP}} = +4.9$ kV), and the MCP input surface had a potential of +2.3 kV. Secondary electrons emitted from the carbon foil consequently enter the MCP with an

energy of 300 eV. The sensor unit for ions can also measure ions by applying the same voltage ($V_{MCP} = +4.9$ kV), while the detection efficiency is lower when secondary electrons enter the MCP with an energy of 4.3 keV. Table 1 summarizes the applied voltages for the LEP experiment. It should be noted that to improve the detection efficiency for the ion measurement, the applied voltage was actually lowered to +2.7 kV ($V_{MCP} = +2.7$ kV) for the ion sensor unit, so that the potential of the MCP incident surface was 0 V and the incident energy of the secondary electrons was 2 keV.

Performance

The performance of the top-hat ESA was calculated using an ISAS electrostatic field modeling program that has been used for the development of several space plasma analyzers for the Kaguya mission (Saito et al. 2008, 2010; Yokota et al. 2005), the Bepi-Colombo mission (Delcourt et al. 2009; Delcourt et al. 2016), the Magnetospheric multiscale (Pollock et al. 2016), and the Martian moons exploration mission (Yokota et al. 2021). In the simulation, the ion trajectories were calculated with $V_{Swp} = -1$ kV and $V_{Fix} = -2$ kV. Because the calculation results for ions are equivalent to that for the electron case when all electric polarities are reversed, the calculation for electrons was omitted.

Figure 4 shows the energy-elevation responses of the top-hat ESA of the LEP experiment derived from a numerical simulation (a) and measured (b) in the laboratory. The dimensions of the top-hat ESA are shown in Fig. 2. Although the simulation assumes ‘detection’ if the incident particle reaches the carbon foil, the two responses agree with each other. The performance of the top-hat ESA estimated by the simulation is summarized in Table 2.

For the SS520-3 rocket observation experiment, we obtained all calibration data, conducting the performance test for all channels of the two sensor units of the LEP experiment. The two sensor units were calibrated at the ISAS facility that has ion beams with well-defined energy

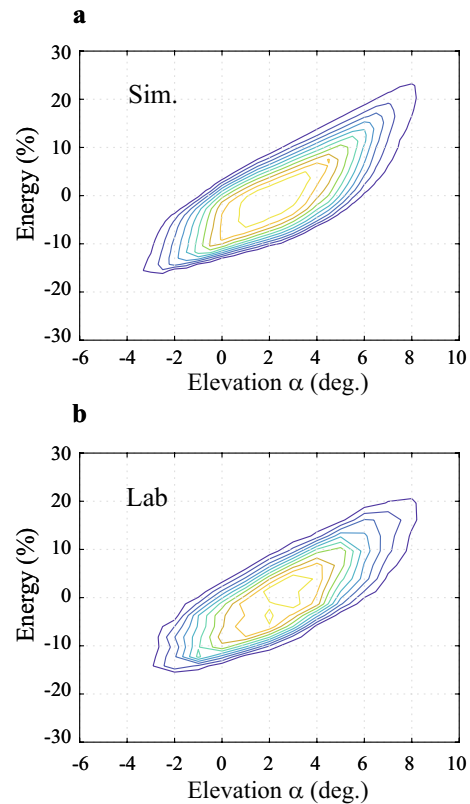


Fig. 4 Energy-elevation responses of the top-hat ESA of the LEP experiment derived from **a** a numerical simulation and **b** measured in the laboratory

and uniform intensity over the sensor aperture. The elevation and azimuth angles of the incident beam were controlled by a multi-axis turntable system in a vacuum chamber (see Fig. 3f). We corrected for time variation in beam intensity using the results of tests conducted at one channel at frequent intervals. Since no equivalent electron beams were available, we used ion beams to calibrate both the electron sensor unit and the ion sensor

Table 1 Applied voltages for ion and electron measurement by the LEP experiment

Parameters	Ion (V)	Electron (V)
HVPS1		
V_{Swp}	0 to -2 k	0 to +2 k
V_{Fix}	-2 k	+2 k
HVPS2		
V_{MCP}	+4.9 k (actually +2.7 k)	+4.9 k
Input surface	+2.3 k (actually 0)	+2.3 k

The potential of the MCP input surface is distributed by a voltage divider

Table 2 Performance of the top-hat ESA of the LEP experiment

Parameters	Simulation	Measurement in Lab (Ion/electron)
g-factor/22.5° channel	5.3×10^3 cm ² sr eV/eV	3.4×10^3 cm ² sr eV/eV 3.2×10^3 cm ² sr eV/eV
Angular res. $\Delta\theta$	6.5° (FWHM)	6.0° (FWHM) 6.1° (FWHM)
Average elevation (θ)	1.1°	0.52° 0.73°
Energy res. $\Delta K/K$	19.2% (FWHM)	18.3% (FWHM) 18.6% (FWHM)
Analyzer const. (K)/V	3.95	4.04 4.00

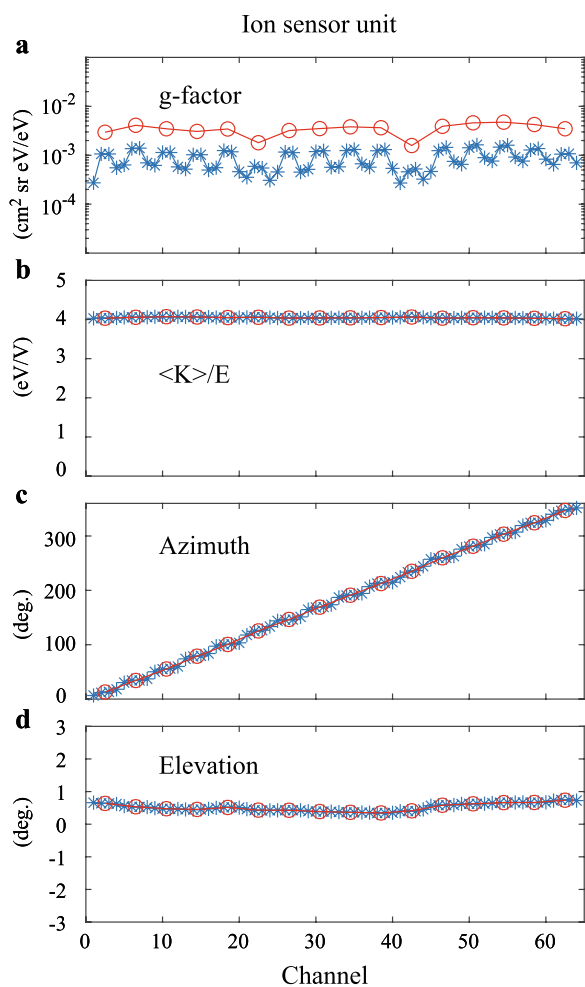


Fig. 5 Characteristics of the ion sensor unit of the LEP experiment measured in the performance tests, **a** g-factor, **b** average energy per inner ESA voltage (analyzer constant), **c** average azimuth, and **d** average elevation

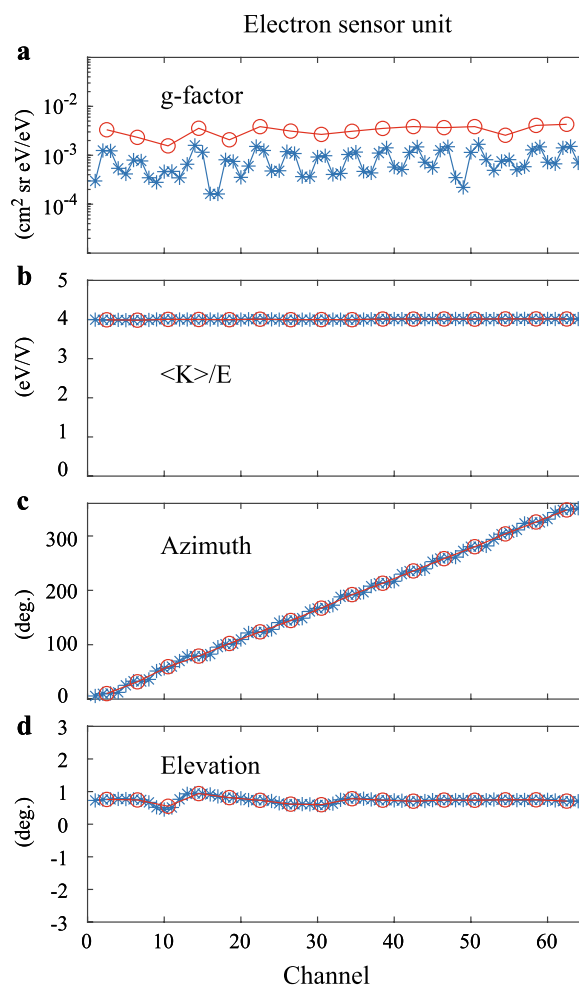


Fig. 6 Characteristics of the electron sensor unit of the LEP experiment measured in the performance tests, **a** g-factor, **b** average energy per inner ESA voltage (analyzer constant), **c** average azimuth, and **d** average elevation

unit. Therefore, we applied exactly the same voltage to the electron sensor unit as to the ion sensor unit during the performance test.

Figures 5 and 6 show g-factor (a), average energy per ESA voltage $\langle K \rangle / V$ (analyzer constant) (b), average azimuth (c), and average elevation $\langle \theta \rangle$ (d) for ion and electron sensor units measured in the performance test, respectively. The ion beam was injected into the sensor unit every 0.5° elevation and every $360^\circ / 128 = 2.8125^\circ$ azimuth to obtain the energy-angular responses for the two sensor units. It should be noted that the three columns at the entrance aperture (see Fig. 3a) and the 16-segmented carbon foil holders (see Fig. 3b) are obstacles depending on the azimuth.

In the laboratory, 64 channels of data were obtained from the 64-channel anode board of the MCP-based detector, and thus the characteristics for 64 channels

were calculated (blue asterisks). However, we calculated 16-channel characteristics (red circles) using the 64 channels of data to use as calibration data, because the onboard 64-channel observation data are processed into 16-channel data by adding 4 channels each. The g-factor distributions of the two sensor units have troughs every 4 channels due to the effect of the carbon-foil holder (see Fig. 3b), while the 16-channel g-factors are approximately constant, slightly affected by the three columns at the entrance aperture. The analyzer constants and elevation responses are very uniform over all channels, indicating that the top-hat ESAs were manufactured and assembled with good axisymmetry. Azimuthal responses vary as expected for the channels.

We used simple electron beam created by a number of tungsten filaments to verify the sensitivity of the electron sensor to electrons. The tungsten filaments were placed

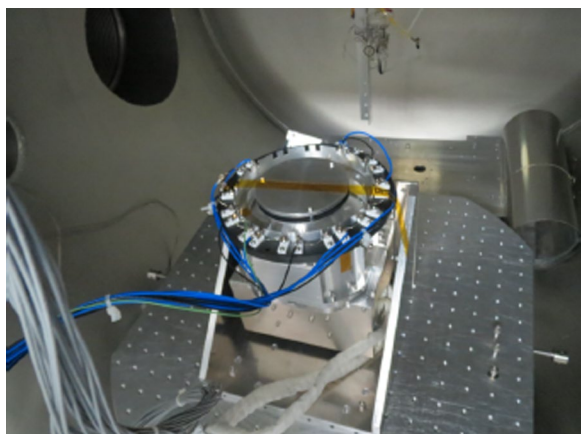


Fig. 7 Photograph of the test of the electron sensor unit of the LEP experiment using an electron beam from filaments

close/near the sensor aperture and were powered/biased individually to emit thermal electrons, as shown in Fig. 7. We confirmed that all channels of the electron sensor unit detected electrons at the potential configuration described in Sect. “Instrumentation”. In the test, a few 100 V were applied to the filament and the incident energy of the electrons was a few 100 eV.

Observation results

The SS-520–3 sounding rocket was launched from Svalbard Rocket Range, Ny- Ålesund in Norway, on November 4, 2021. Figure 8 shows energy-time spectra of ions and electrons measured by the LEP experiment during the observation experiment (the launch at $X = 0$ s). The two spectra were derived from the observation

data of the four channels that pointed upward during the observation and consequently detected ions and electrons in the downward direction. The ion energy-time spectrum shows that ions of a few 100 eV increase in flux with time, gradually decreasing in energy from $X = 700$ s, and increasing in energy from $X = 750$ s. Such energy variations have also been observed by the SS520-2 rocket and have been explained as corresponding to the Invariant Latitude (ILAT) variation of the rocket trajectory (Tanaka et al. 2003). This means that the rockets observed the effect of velocity filtering due to convection in the anti-solar direction in the polar region (Reiff et al. 1977). Although the highest altitude of the SS520-3 rocket flight was 756 km at $X = 490$ s, lower than that of the SS520-2 rocket (1040 km), the firing azimuths were both around 200° . Therefore, the energy-time spectra measured by the LEP experiment include phenomena and structures similar to those observed by the SS520-2 rocket (Tanaka et al. 2003).

The electron energy-time spectrum in Fig. 8a shows several inverted-V type precipitations, maximum energies of which are around a couple of 100 eV. Such low-energy inverted-V electron precipitation frequently appeared in the dayside auroral region (Newell et al. 1991). The ion precipitation disappeared when the inverted V-shaped electron precipitation was observed. This is probably due to the fact that the field-aligned electric field accelerated the electrons, while the ions were blocked from precipitating (Reif et al. 1993). All of the above features in the ion and electron spectra were also reported in the SS520-2 observations (Tanaka et al. 2003).

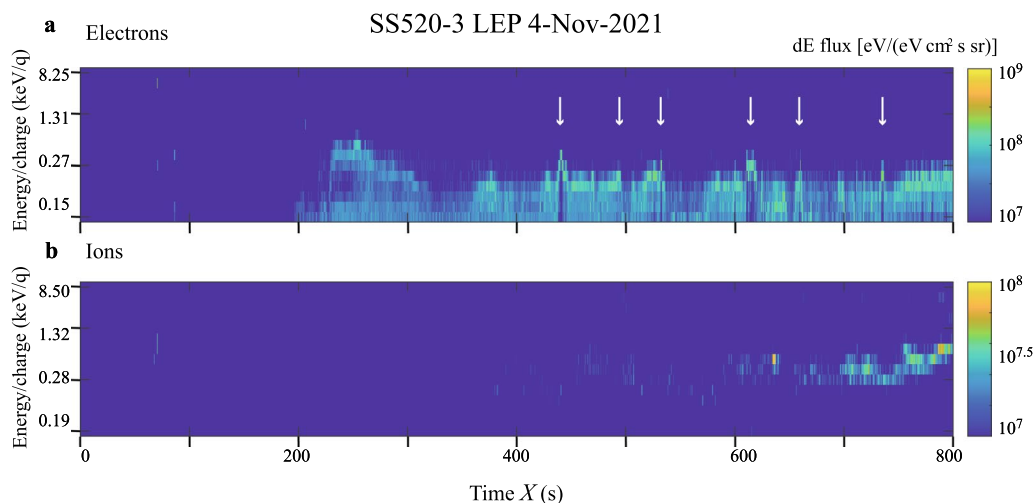


Fig. 8 Energy-time spectra of **a** ions and **b** electrons measured by the LEP experiment during the observation experiment of the SS520-3 rocket on November 4, 2021. White arrows indicate the timings for the inverted-V electron precipitations

Summary

We developed a sensor head that can measure both ions and electrons. Two identical sensor units of the LEP experiment, one for ions and the other for electrons, were manufactured for the SS520-3 rocket program. The observation data obtained by the LEP experiment on the SS520-3 rocket shows typical characteristics and structures of the polar cusp region, similar to previous observations made by the SS520-2 rocket. The data of the LEP experiment are now being analyzed in detail with data from other instruments on the SS520-3 rocket to achieve the science objectives.

The LEP experiment developed in this study has proven to be comparable in performance to conventional ion and electron analyzers. Although several analyzers that measure both ions and electrons have been reported (Frank et al. 1992; McFadden et al. 2008; Kasper et al. 2016; Su et al. 2022, Hirahara, Takei et al. 2023), the advantage of the LEP experiment is that the additional resource is only carbon foils. In future, the LEP experiment will be used not only for multi-point plasma observations, but also for solar system exploration. We have experienced a couple of exploration programs which employed an ion mass analyzer. If this technique of the LEP experiment had been established, it would have been possible to switch to electron measurement.

Abbreviations

ASIC	Application specific integrated circuit
ESA	Electrostatic analyzer
FOV	Field-of-view
FWHM	Full width at half maximum
HK	Housekeeping
HVPS	High-voltage power supply
ILAT	Invariant Latitude
ISAS	Institute of Space and Astronautical Science
LEP	Low-energy particle
MCP	Micro-channel plate
SRIM	Stopping and Range of Ions in Matter

Supplementary Information

The online version contains supplementary material available at <https://doi.org/10.1186/s40623-024-01997-7>.

Additional file 1: Figure S1. Flags in the HK data of the LEP experiment during the observation experiment by the SS-520-3 rocket, a) HVPS on, b) Motor drive, c) Not Sensor in extended position and d) Not Sensor in stowed position. Red and blue circles indicate the flags for the ion and electron sensor units, respectively.

Acknowledgements

The authors would like to express sincere thanks to all members of the SS520-3 rocket program. The experiment was manufactured by Mitaka Kohki Co., Ltd. and Meisei Electric Co., Ltd. This study was supported by ISAS/JAXA as a collaborative program with the Space Chamber Laboratory and the joint research program of the Institute for Space—Earth Environmental Research (ISEE), Nagoya University.

Author contributions

SY wrote the manuscript. SY, YS, and KA contributed to the development of the experiment, observation by SS520-3 sounding rocket, and processing of the observation data.

Funding

This research was partially supported by a Grant-in-Aid for Scientific Research from the Japan Society for the Promotion of Science (#20K04039, #17H01164, #26287121, #21H04509, #21H04526).

Availability of data and materials

The data and materials used in this research are available on request to the corresponding author, Dr. Shoichiro Yokota (yokota@ess.sci.osaka-u.ac.jp).

Declarations

Ethics approval and consent to participate

Not applicable.

Consent for publication

Not applicable.

Competing interests

The authors declare that they have no competing interests.

Author details

¹Osaka University, Machikaneyama-cho, Toyonaka 560-0043, Japan. ²Institute of Space and Astronautical Science, Japan Aerospace Exploration Agency, Yoshinodai, Chuo-ku, Sagami-hara 252-5210, Japan.

Received: 1 September 2023 Accepted: 22 March 2024

Published online: 06 April 2024

References

- Asamura K, Kazama Y, Yokota S, Kasahara S, Miyoshi Y (2018) Low-energy particle experiments—ion analyzer (LEPI) onboard the ERG (Arase) satellite. *Earth Planets Space* 70:70. <https://doi.org/10.1186/s40623-018-0846-0>
- Barabash S et al (2013) Particle Environment Package (PEP). Vol. 8, EPSC2013-709, 2013 European Planetary Science Congress 2013. <https://meetingorganizer.copernicus.org/EPSC2013/EPSC2013-709.pdf>
- Burch JL, Goldstein R, Cravens TE, Gibson WC, Lundin RN, Pollock CJ, Winningham JD, Young DT (2007) RPC-IES: the ion and electron sensor of the rosetta plasma consortium. *Space Sci Rev* 128:697–712. <https://doi.org/10.1007/s11214-006-9002-4>
- Carlson CW, Curtis DW, Paschmann G, Michel W (1982) An instrument for rapidly measuring plasma distribution functions with high resolution. *Adv Sp Res* 2(7):67–70
- Delcourt D et al (2009) The mass spectrum analyzer (MSA) onboard BEPI COLOMBO MMO: scientific objectives and prototype results. *Adv Space Res* 43:869–874. <https://doi.org/10.1016/j.asr.2008.12.002>
- Delcourt D et al (2016) The mass spectrum analyzer (MSA) on board the Bepi-Colombo MMO. *J Geophys Res Space Phys* 121(7):6749–6762. <https://doi.org/10.1002/2016JA022380>
- Frank LA, Ackerson KL, Lee JA, English MR, Pickett GL (1992) The plasma instrumentation for the Galileo mission. *Space Sci Rev* 60:283–304
- Fraser GW (2002) The ion detection efficiency of microchannel plates (MCPs). *Int J Mass Spectrom* 215:13–30. [https://doi.org/10.1016/S1387-3806\(01\)00553-X](https://doi.org/10.1016/S1387-3806(01)00553-X)
- Galli A, Vorburger A, Carberry Mogan SR, Roussos E, Stenberg Wieser G, Wurzel P et al (2022) Callisto's atmosphere and its space environment: prospects for the particle environment package on board JUICE. *Earth Space Sci*. <https://doi.org/10.1029/2021EA002172>
- Hirahara M, Takei T, Yokota S, Yanagimachi T (2023) Triple-dome electrostatic energy analyzer with 360-deg. field-of-view for simultaneous

- measurements of ions and electrons. *J Geophys Res.* <https://doi.org/10.1029/2023JA031423>
- Kasahara S, Tao R, Yoshida E, Yokota S (2023) A two-stage deflection system for the extension of the energy coverage in space plasma three-dimensional measurements. *Earth Planets Space* 75:91. <https://doi.org/10.1186/s40623-023-01845-0>
- Kasper JC et al (2016) Solar wind electrons alphas and protons (SWEAP) investigation: design of the solar wind and coronal plasma instrument suite for solar probe plus. *Space Sci Rev* 204:131–186
- McFadden JP et al (2008) The THEMIS ESA plasma instrument and in-flight calibration. *Space Sci Rev* 141:227–302
- Morel X, Berthomier M, Berthelier JJ (2016) Electrostatic analyzer with a 3-D instantaneous field of view for fast measurements of plasma distribution functions in space. *J Geophys Res Space Phys* 122:3397–3410. <https://doi.org/10.1002/2016ja023596>
- Ogasawara K et al (2018) A double-cusp type electrostatic analyzer for high-cadence solar-wind suprathermal ion observations. *Rev Sci Instrum* 89:114503
- Patrick T, Newell William J, Burke Ching-I, Meng Ennio R, Sanchez Marian E, Greenspan (1991) Identification and observations of the plasma mantle at low altitude. *J Geophys Res: Space Physics* 96(A1) 35–45. <https://doi.org/10.1029/90JA01760>
- Pfaff RF, Borovsky JF, Young DT (eds) (1998) Measurement techniques in space plasmas: particles. American Geophysical Union, Washington
- Pollock C et al (2016) Fast plasma investigation for magnetospheric multiscale. *Space Sci Rev* 199(1):331–406. <https://doi.org/10.1007/s11214-016-0245-4>
- Reiff PH, Burch JL, Hill TW (1977) Solar wind plasma injection at the dayside magnetospheric cusp. *J Geophys Res* 82:49–491
- Reiff PH, Lu G, Burch JL, Winningham JD, Frank LA, Craven JD, Peterson JD, Hoffman RA (1993) On the high-and low-altitude limits of the auroral electric field region. In: Lysak RL (ed) Geophysical monograph. AGU, Washington D C, pp 143–154
- Saito Y et al (2008) Low energy charged particle measurement by MAP-PACE onboard SELENE. *Earth Planets Space* 60:375–385. <https://doi.org/10.1186/BF03352802>
- Saito Y et al (2010) In-flight performance and initial results of plasma energy angle and composition experiment (PACE) on SELENE (Kaguya). *Space Sci Rev* 154(1–4):265–303. <https://doi.org/10.1007/s11214-010-9647-x>
- Saito Y, Yokota S, Asamura K (2017) High speed MCP anodes for high time-resolution low-energy charged particle spectrometers. *J Geophys Res* 122(2):1816–1830. <https://doi.org/10.1002/2016JA023157>
- Saito Y et al (2021) Pre-flight calibration and near-earth commissioning results of the mercury plasma particle experiment (MPPE) onboard MMO (Mio). *Space Sci Rev* 217:70. <https://doi.org/10.1007/s11214-021-00839-2>
- Sauvaud JA, Delcourt D, Parrot M, Payan D, Raita T, Penou E (2018) Low-altitude observations of recurrent short-lived keV ion microinjections inside the diffuse auroral zone. *J Geophys Res Space Phys* 123:2054–2063. <https://doi.org/10.1002/2017JA025075>
- Spicher A, Ilyasov AA, Miloch WJ, Chernyshov AA, Clausen LBN, Moen JI, Abe T, Saito Y (2016) Reverse flow events and small-scale effects in the cusp ionosphere. *J Geophys Res Space Phys* 121:10466–10480. <https://doi.org/10.1002/2016JA022999>
- Su B, Kong LG, Zhang AB, Tian Z, Wang WJ, Lv YL, Ma LY (2022) The bipolar charge plasma spectrometer (BCPS) based on the 2 π -field-of-view double-channel electrostatic analyzer. *Rev Sci Instrum* 93:043305. <https://doi.org/10.1063/5.0082410>
- Tanaka H, Saito Y, Ishii S, Asamura K, Mukai T (2003) Simultaneous observation of the electron acceleration and ion deceleration in the dayside high-latitude auroral region. *Geophys Res Lett* 30(12):1615. <https://doi.org/10.1029/2003GL017071>
- Yokota S, Saito Y, Asamura K, Mukai T (2005) Development of an ion energy mass spectrometer for application on board three-axis stabilized spacecraft. *Rev Sci Instrum* 76:014501–014508
- Yokota S, Kasahara S, Mitani T, Asamura K, Hirahara M, Takashima T, Yamamoto K, Shibano Y (2017) Medium-energy particle experiments – ion mass analyzer (MEP-i) onboard ERG (Arase). *Earth Planets Space* 69:172. <https://doi.org/10.1186/s40623-017-0754-8>
- Yokota S et al (2021) In situ observations of ions and magnetic field around Phobos: the mass spectrum analyzer (MSA) for the Martian Moons eXploration (MMX) mission. *Earth Planets Space* 73:216. <https://doi.org/10.1186/s40623-021-01452-x>
- Young DT, Bame SJ, Thomsen MF, Martin RH, Burch JL, Marshall JA, Reinhard B (1988) 2 π -radian field-of-view toroidal electrostatic analyzer. *Rev Sci Instrum* 59:743
- Ziegler JF (2004) SRIM-2003. *Nucl Instrum Meth Phys Res B* 219–220:1027–1036

Publisher's Note

Springer Nature remains neutral with regard to jurisdictional claims in published maps and institutional affiliations.